

UDK 514.124.7:553.689

Mechanical-Chemical Synthesis $Ba_{0.77}Sr_{0.23}TiO_3$

D. Kosanović^{1*)}, N. Obradović¹, J. Živojinović¹, S. Filipović¹,
A. Maričić², V. Pavlović¹, Y. Tang³, M. M. Ristić⁴

¹Institute of Technical Sciences of the Serbian Academy of Sciences and Arts,
Knez Mihailova 35/IV, 11000 Belgrade, Serbia

²Technical Faculty of Čačak, University of Kragujevac, Svetog Save 65, 32000 Čačak, Serbia

³North Carolina Central University Durham, USA

⁴Serbian Academy of Sciences and Arts, Knez Mihailova 35, 11000 Belgrade, Serbia

Abstract:

Barium-Strontium-Titanate $Ba_{0.77}Sr_{0.23}TiO_3$ was prepared from starting materials $BaCO_3$, $SrCO_3$ and TiO_2 through solid-state reactions. Mixtures of these oxides are mechanically activated in a high-energy planetary ball mill at different time intervals from 0 to 120 minutes. In order to obtain information on phase composition, crystal structure was determined by X-ray diffraction. It was observed that after 80 minutes in process synthesis $Ba_{0.77}Sr_{0.23}TiO_3$ started. Thermal analyzes were performed in order to determine the characteristic temperatures of the processes that occur in the solid phase. Particle size distribution, together with electron microscopy scanning has given us very useful information about the morphology of the powder.

Keywords: Mechanical activation, Scanning electron microscopy, Crystal structure, Barium-strontium-titanate.

1. Introduction

Barium-strontium-titanate, $Ba_{1-x}Sr_xTiO_3$, (BST) is a ferroelectric material with a tetragonal structure at room temperature for $x < 3$, which has a perovskite structure (ABO_3) [1]. BST is a solid solution composed of titanate, barium-titanate ($BaTiO_3$) and strontium-titanate ($SrTiO_3$). $BaTiO_3$ is a ferroelectric material with Curie temperature (T_C) of 120°C, while the $SrTiO_3$ is Para electric material with non-ferroelectric phase transformations. At room temperature for the solid solution in ferroelectric phase Ba content is in the range of 0.7 to 1.0, while the content of Ba in paraelectric phase is less than 0.7. There are several methods for the synthesis of $Ba_{1-x}Sr_xTiO_3$ powder, either with dry or wet chemical way of synthesis. The first ones, based on reactions in the solid state, are the most widely used methods for obtaining a BST, while the other methods are co-precipitation, spray pyrolysis, and sol-gel techniques used by Wechsler, Kirby and Thakur [2-5]. Among them, there are hydrothermal techniques that are commercially used for production of given material by Miao and Zhou [6]. Each of these methods has its advantages and disadvantages. Some of the advantages are high purity, super fine powder production, good fluidity, low agglomeration and lower sintering temperatures.

Disadvantages of the above mentioned techniques are high-temperature calcinations

*) Corresponding author: darko.kosanovic@itn.sanu.ac.rs

(from 1000°C to 1200°C), followed by the use of larger amounts of the initial powder, as well as large grain size which can not be used for production of materials with high dielectric constant.

In our research, we focused on influence of mechanical activation on the formation of single phase $\text{Ba}_{0.77}\text{Sr}_{0.23}\text{TiO}_3$. This method was performed since it provides better homogeneity of the starting powders, and because it is relatively simple and economical. Also, some of the techniques used are the advantages of low calcinations temperature ($T = 800^\circ\text{C}$) and low temperature sintering to obtain the desired compounds.

2. Experimental procedure

Within our study, for synthesis of $\text{Ba}_{0.77}\text{Sr}_{0.23}\text{TiO}_3$ system following powders BaCO_3 (99,8% p.a. Aldrich), SrCO_3 (99,8% p.a. Aldrich) and TiO_2 (99,99% p.a. Aldrich) were used. Initial mixtures were ground in a zirconium-oxide container (volume 500 cm^3), together with balls of 10 mm diameter (the ratio of powder and ball was 1:20). Mechanical activation of starting powders was performed in high-energy planetary ball mill (Retsch, AM 400) in time intervals of 0, 5, 10, 20, 40, 80 and 120 minutes, with presence of atmospheric air. The powders were categorized from BST to GMT-0-120, depending on the time of activation.

Crystal phase of starting powders is determined by using diffractogram of powder (Philips PW 1050) with $\lambda\text{CuK}\alpha$ radiation. Tests were performed at room temperature in the range of angles $10\text{-}80^\circ$ (2θ) with step of $0,05^\circ$ and the retention time of 1s per step.

The median particle size (PSA), particle size distribution, and the nature of the agglomerates in mechanically activated BST powders were determined by using a laser particle size analyzer (Mastersizer 2000, Malvern Instruments Ltd., United Kingdom). This instrument covers the interval of particle sizes from 20 nm to 2 mm. During the measurement, the particles were dispersed in isopropanol. For PSA measurements, powders were mixed with distilled water in an ultrasonic bath.

DTA and TG analysis of the system $\text{BaCO}_3\text{-SrCO}_3\text{-TiO}_2$ were performed on the device SDT Q600 V20.9 Build 20, from room temperature to 1100°C . 25 mg of powder was taken at the time for analysis. Analyses were performed in an atmosphere saturated with nitrogen, N_2 . Analyses were performed on not activated powder, as well as powder activated at 5, 10, 20, 40, 80 and 120 minutes, with heating rate increase of $10^\circ\text{C}/\text{min}$.

Tests for particle morphology and microstructure of mechanically activated BST powders were performed by using Scanning Electron Microscop (SEM, JSM-6390 LV JEOL, 25kV).

3. Results and Discussion

Powder diffraction patterns of mechanically activated and inactivated mixtures (GMT-0 GMT-5, BST-10 BST-20 BST-40 BST-80 BST-120) are shown in Fig. 1. Presented results correspond to diffractograms of mechanically activated mixtures BaCO_3 , TiO_2 (anatase) and SrCO_3 , while identification of all reflections obtained was performed by using JCPDS Cards (47-1488 for BaO , 73-1764 for $\text{TiO}_2\text{-a}$, 41-0373 for BaCO_3 , 74-11491 for SrCO_3 , 77-1566 for $\text{Ba}_6\text{Ti}_{17}\text{O}_{40}$, 44-0093 for $\text{Ba}_{0.77}\text{Sr}_{0.23}\text{TiO}_3$).

Initial powder diffraction patterns (BST-0) indicates a narrow and sharp peaks of high intensity, which points to their initial crystalline state. After 5 and 10 min of mechanical activation, process leads to reduction of peak intensity and there is no change in phase composition. It has been observed that after 20 min of mechanical activation there is still no change in phase composition and appearance of new phases, but amorphization of powder was spotted, which is henceforth reflected in further reduction of spread and intensity of the

reflection. In addition, we observed a different relationship between the intensity peaks. Furthermore, a different relationship between the intensity of peaks was observed.

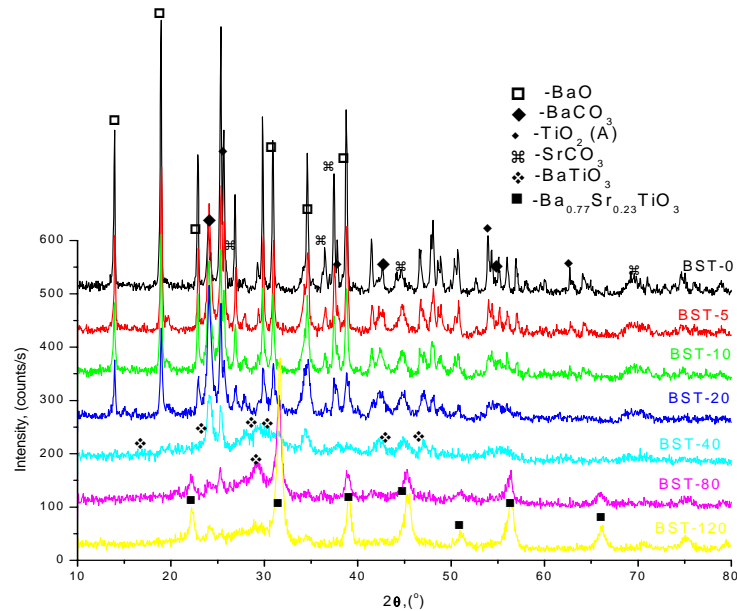


Fig. 1. Diffraction patterns of activated and inactivated powders

Only after 40 minutes of mechanical activation, process leads to the appearance of new phases of barium-titanate (BaTiO_3). 80 minutes of mechanical activation leads to the emergence of another new phase $\text{Ba}_{0.77}\text{Sr}_{0.23}\text{TiO}_3$. Beside $\text{Ba}_{0.77}\text{Sr}_{0.23}\text{TiO}_3$ in the mixture, BaTiO_3 and TiO_2 are present in small quantities and finally after 120 min of mechanical activation almost pure phase $\text{Ba}_{0.77}\text{Sr}_{0.23}\text{TiO}_3$ is obtained.

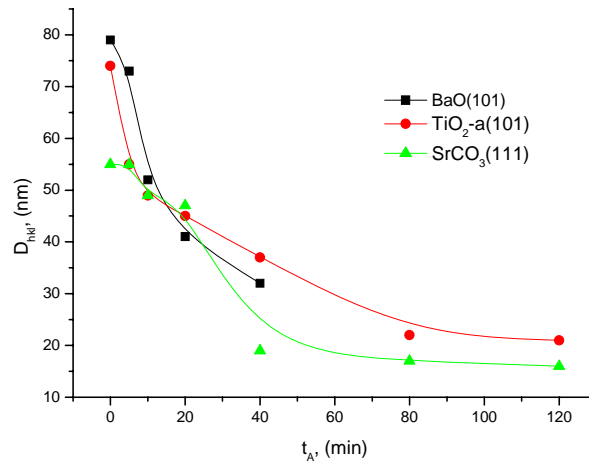


Fig. 2. Dependency of average crystallite dimensions D_{hkl} of the activation time for the BaO (101), TiO_2 (101) and SrCO_3 (111).

With an X-ray diffraction of samples, characteristic reflection of Bragg diffraction angles (2θ), intensities of their corresponding peaks (I), as well as line width diffraction on the half-height (β) and mutual distance (d), are finally obtained. Based on these data we calculated following parameters: the size of coherent scattering domains (average crystallite size, D_{hkl}), the minimum density of dislocations (ρ_D) and microstrain (ϵ_{hkl}). Fig. 2 shows the graph of time activation dependency of the average crystallite dimensions D_{hkl} for the BaO (101),

TiO₂(101) and SrCO₃(111). From the following graph it is clearly noticeable that, up to 40 minutes of activation, more significant fragmentation takes place first with powder BaO and TiO₂, which are softer than the SrCO₃ so they react with each other. After that time, barium oxide disappears, fragmentation of strontium-carbonate continues and further continuous fragmentation of titanium-dioxide takes place. For all powders with prolongation of mechanical activation crystallite size (D_{hkl}) decreases.

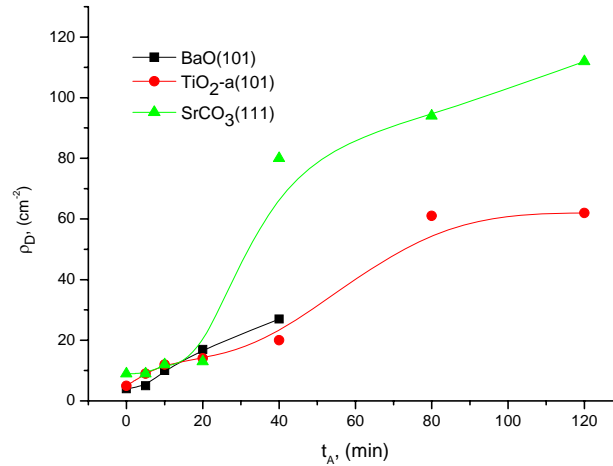


Fig. 3. Dependence of density dislocation ρ_D of the activation time for the BaO(101), TiO₂(101) and SrCO₃(111)

Fig. 3 shows graph of dependency of density dislocation ρ_D the activation time for the BaO(101), TiO₂(101) and SrCO₃(111). It is observed that with BaO (101), TiO₂ (101) and SrCO₃ (111) minimum density dislocation ρ_D increases with prolongation of mechanical activation.

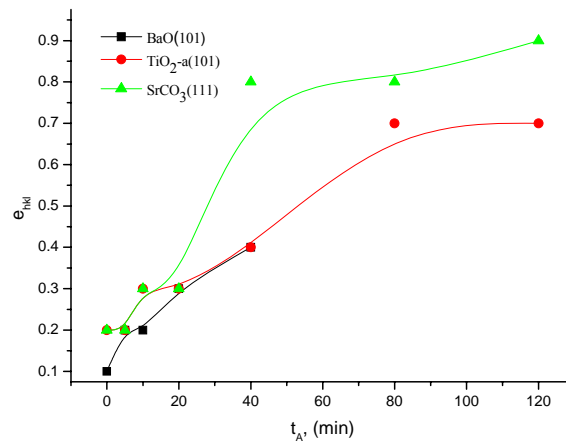


Fig. 4. Microstrain dependence e_{hkl} of the activation time for BaO(101), TiO₂(101) and SrCO₃(111)

Fig 4 shows graph of microstrain dependency e_{hkl} of the activation time for the BaO (101), TiO₂ (101) and SrCO₃ (111). It is observed that in BaO (101), TiO₂ (101) and SrCO₃ (111) the intensity of microstrain increases with prolonged time of mechanical activation. Based on these diffraction patterns and calculated structural parameters, as well as a detailed review of the literature [7], the mechanism of barium-strontium-titanate formation is proposed. The reaction of barium-carbonate and titanium-dioxide creates BaTiO₃ along with separation of carbon dioxide. Due to the excess of titanium-dioxide (which has not yet reacted

with strontium-carbonate), the obtained BaTiO_3 reacts with titanium dioxide creating intermedial compound $\text{Ba}_6\text{Ti}_{17}\text{O}_{40}$ [8]. Then, this compound reacts with strontium-carbonate $\text{Ba}_{0.77}\text{Sr}_{0.23}\text{TiO}_3$ along with the separation of carbon dioxide. The reaction mechanism is proposed in the following three stages:

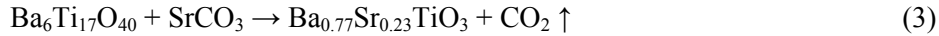


Fig. 5 shows micrographs of initial mechanically inactivated and activated powders in 5, 10 and 20 minutes, with a magnification of 5,000 times. SEM micrograph of initial powder, Fig. 5 (a), shows us the mixture of powders to form soft agglomerates whose size is about 10 microns. It is also visible that the finer particles have twined the larger ones.

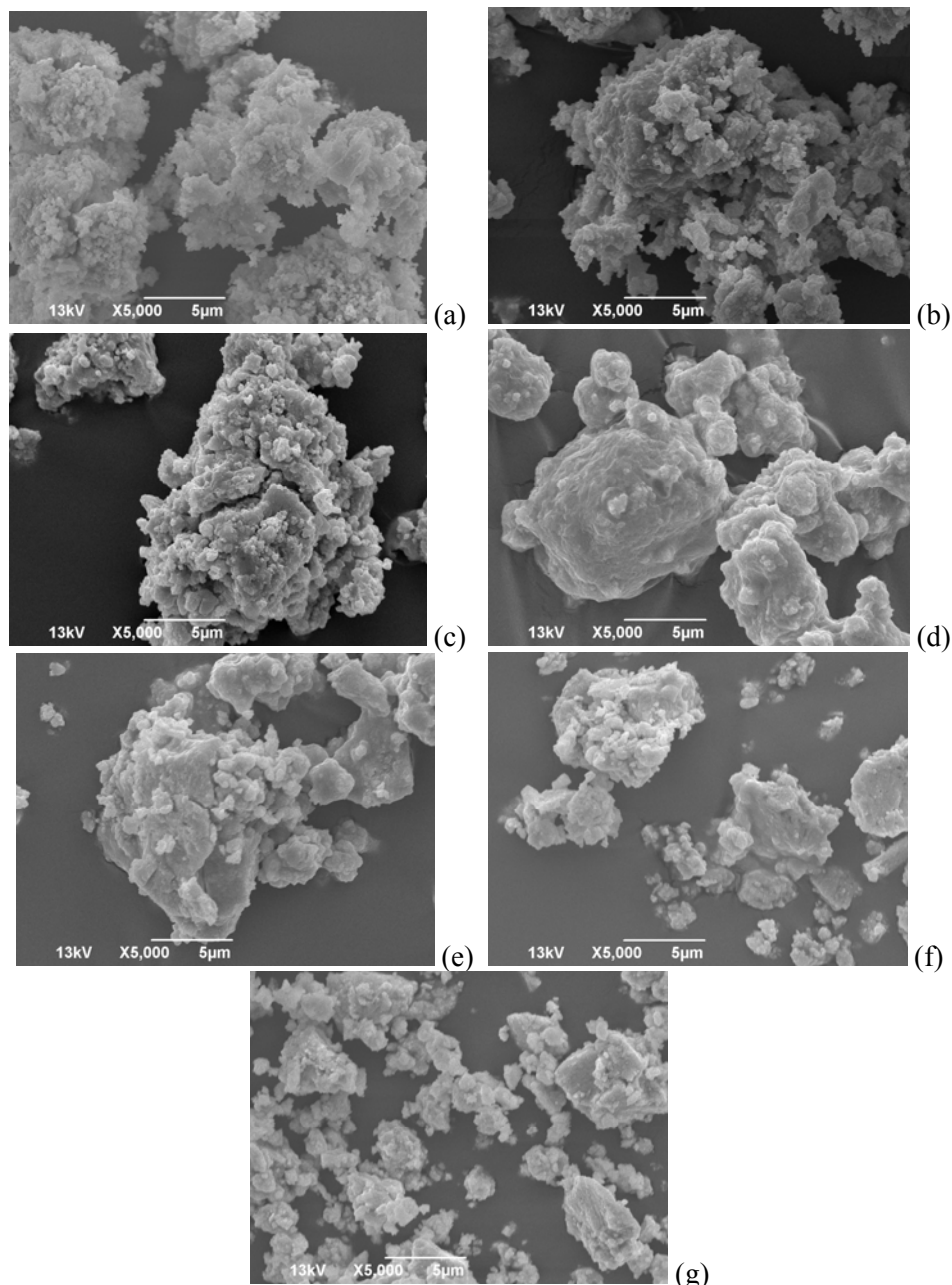


Fig. 5. Electronically scanned micrographs of starting powders (a) B-0, (b) BST-5, (c) BST-10, (d) BST-20, (e) BST-40, (f) and BST-80 (g) BST-120.

After 5 min of mechanical activation, Fig. 5 (b), fragmentation of larger particles and agglomerates takes place. Surface activity of small particles is increasing, which leads to their clustering around larger ones. Therefore, agglomerates themselves are smaller and softer. Significant erosion of the surface of particles is also evident. Particle size after five minutes of activation is between 7 and 8 μm . With prolonged mechanical activation, Fig. 5 (c) and (d), an additional refinement and strengthening of agglomerates is present. Appearance of two types of agglomerate of size 4-5 and 8 μm is evident. Fig. 5 (e), (f) and (g), shows the micrographs of powders mechanically activated 40, 80 and 120 minutes. New phases are noticeable, as well as drastic reduction of the initial particle size. As a result of mechanical activation there is mass transport processes between the contact surfaces. This causes rearrangement of existing, and formation of a new phase on the surface of particles. The process is accompanied by agglomeration of smaller particles into larger, as well as the emergence of erosion of the surface of the new phase that is stronger than other components.

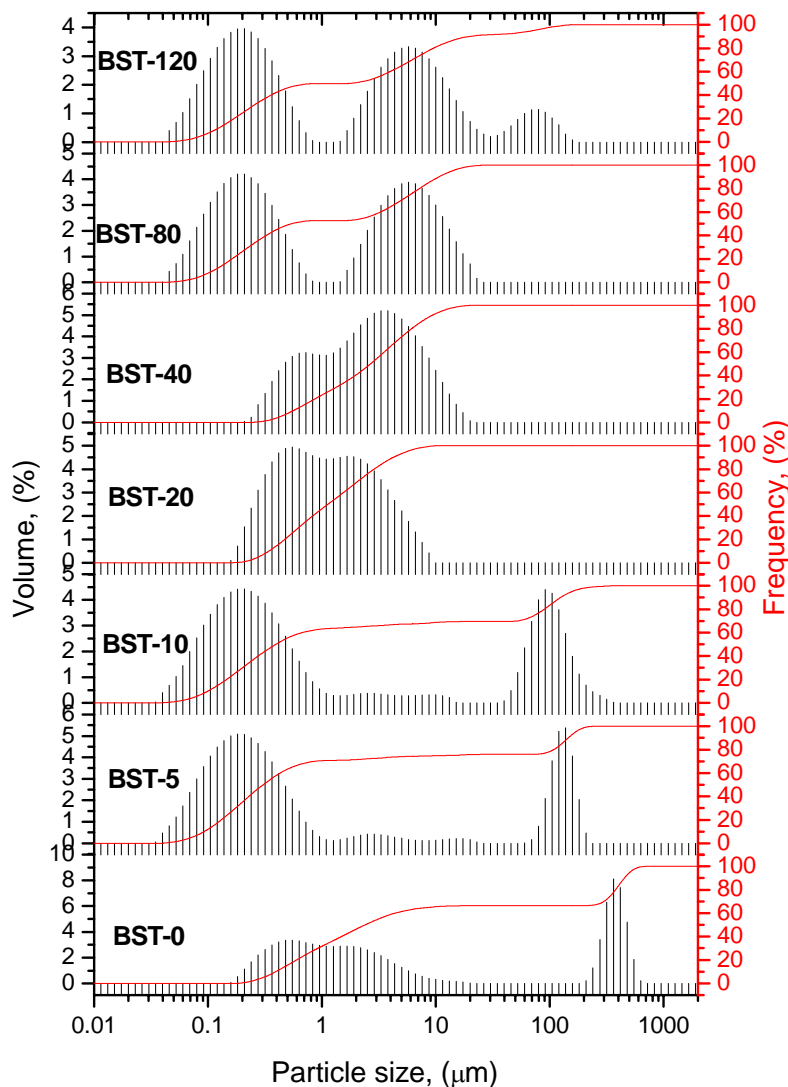


Fig. 6. Particle size distribution in the BST powders

Figs. 6 shows particle size distribution and cumulative distribution curve for all samples BST. Fig. 6 shows that BST-0 particle size distribution consist of two fractions

(bimodal distribution). Those are, a fraction with two folds, i.e. two humps with particle sizes of 0.5 μm (corresponding to SrCO_3), 2 μm (corresponding to TiO_2) and other fractions corresponding to BaCO_3 particle size of about 400 μm . Mechanical activation of 5 and 10 minutes farther shows us two groups of particles, or two fractions of about 0.2 and 100 μm . This indicates that there has been a reduction in particle size. After 40 min of mechanical activation (Figs. 6 BST-40) process leads to formation of a re-fraction as well as the appearance of a new phase of BaTiO_3 with larger particles. Further milling of BST powders after 80 minutes led to a additional reduction in particle size and appearance of two factions of 0.19 and about 5.86 μm . First fraction comes from appearance of new phases of BaSrTiO_3 , while other comes from residual barium-titanate (BaTiO_3). After 120 minutes of milling only $\text{Ba}_{0.77}\text{Sr}_{0.23}\text{TiO}_3$ is present but with no significant change in particle size.

Tab. I. Characteristic temperatures of DTA analysis as well as mass changes of all samples

Sample	T ₁ (°C)	T ₂ (°C)	T ₃ (°C)	T ₄ (°C)	T ₅ (°C)	T ₆ (°C)	TG (%)
BST-0	77,97	141,38	639,50	810,75	875,13	936,22	16,39
BST-5	79,28	129,98	638,38	810,75	915,04	939,66	16,45
BST-10	80,73	118,39	606,52	809,30	920,83	954,14	16,17
BST-20	89,42	/	609,41	810,75	910,69	946,90	15,50
BST-40	95,67	/	632,44	809,40	900,83	931,80	13,85
BST-80	91,24	/	/	809,93	877,24	915,58	8,73
BST-120	92,72	/	/	816,54	859,54	911,15	6,10

Differential thermal (DTA) and thermo-gravimetric (TG) analysis were performed to determine characteristic temperatures at which the processes occur in the solid state. All samples were analyzed and the results are shown in Tab. 1, while the results of analysis of BST and BST-0-80 were exposed. In Fig. 7 (a) shows the thermogram of inactivated BST with several endothermic and exothermic peaks. In the temperature range of 58.97°C to 118.88°C, there are two obvious endothermic peaks that are a consequence of separation of moisture and impurities which are absorbed by sample from the atmosphere during preparation. The graph hump in the range 550-650°C is result of crossing the anatase in rutile. Endothermic peak at temperature of 810°C is result of carbonate BaCO_3 [9] decomposition. This trend is further followed by exothermic process initiated by creation of a new phase of BaTiO_3 . This process is accompanied by a mass decrease of about 16%. The fourth endothermic peak on the thermogram is the result of decomposition of SrCO_3 . Two interlinked exothermic peaks over 1000°C point to the creation of $\text{Ba}_{0.77}\text{Sr}_{0.23}\text{TiO}_3$ through the intermediate compound $\text{Ba}_6\text{Ti}_{17}\text{O}_{40}$.

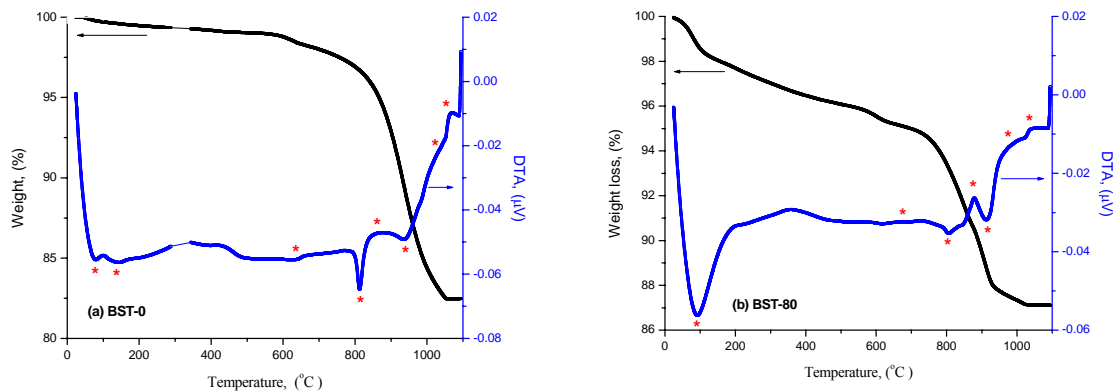


Fig. 7. DTA and TG thermogram (a) BST-0 and (b) BST-80

Fig. 7 (b) shows the thermogram of the powder mechanically activated for 80 minutes, with heat rate increase of 10°C/min. In this graph, endothermic and exothermic peaks of increased width are also observed. Endothermic peak at 800°C is less pronounced because during the mechanical activation most of the carbonate is dissolved and accompanied by a small change in mass decrease of 9 %. Table 1 shows characteristic temperature states for all samples analyzed, as well as mass changes. Naturally, due to the influence of mechanical activation, process lead to spread of some peaks and shifts towards higher temperatures (due to the comminution of powder) for the less activated powders, and then towards lower temperatures (for powders that are activated for a longer time, and where it has already lead to new phase formation as well as agglomerates).

4. Conclusion

In this paper, the influence of mechanical activation on the synthesis of barium-strontium-titanate $\text{Ba}_{0.77}\text{Sr}_{0.23}\text{TiO}_3$ has been examined. Roentgenograms indicate the phase formation of barium-titanate right after 40 minutes of mechanical activation. A new phase and the formation of $\text{Ba}_{0.77}\text{Sr}_{0.23}\text{TiO}_3$ only came after 80 minutes of milling. Given the small amount of intermediate phase $\text{Ba}_6\text{Ti}_{17}\text{O}_{40}$, the phase itself was not detected on roentgenogram. In addition, based on powder diffraction patterns inactivated and mechanically activated 5, 10 and 20 minutes, we got values for the density of dislocations, microstrains and the average dimension of crystallites of BaO , SrCO_3 and TiO_2 . Based on obtained results, we concluded that with increase of mechanical activation time the average crystallite size decreases, while the minimum size of microstrain and dislocation density increases. Also, the proposed mechanism of $\text{Ba}_{0.77}\text{Sr}_{0.23}\text{TiO}_3$ through intermediate compound $\text{Ba}_6\text{Ti}_{17}\text{O}_{40}$.

SEM and PSA confirm results obtained with the X-ray analysis, indicating the fragmentation of initial powder particle size, formation of new phases, as well as smaller particles agglomeration into larger, and appearance of surface erosion of a new phase. DTA and TG analysis has given us a characteristic temperatures for the processes occurring in the system during heating up to 1100°C. Based on these results, the further course of our research will study the sintering of mechanically activated systems $\text{Ba}_{0.77}\text{Sr}_{0.23}\text{TiO}_3$.

Acknowledgment

These studies were performed in the project framework of ON 172057, financed by the Ministry of Education and Science of Republic of Serbia, projects F/198, funded by Serbian Academy of Science and Arts and projects NSF CREST (HRD-0833184) and NASA (NNX09AV07A).

5. References

1. T. W. Tzu, Z. A. Ahmed and A. F. M. Noor. Dielectric Properties Microstructure of $\text{Ba}_{0.70}\text{Sr}_{0.30}\text{TiO}_3$ Derived from Mechanically Activated $\text{BaCO}_3\text{-SrCO}_3\text{-TiO}_2$, Journal of Materials Online, Vol. 2 November (2006), 1.
2. A. Ries, A. Z. Simões, M. Cilense, M. A. Zaghete, J. A. Varela. Barium strontium titanate powder obtained by polymeric precursor method, Materials Characterization 50 (2003), 217.
3. B. A. Wechsler, K. W. Kirby. Phase equilibria in the system barium titanate–strontium titanate, J. Am. Ceram. Soc. 75 (1992), 981.

4. T. Noh, S. Kim, C. Lee. Chemical preparation of barium– strontium-titanate, Bull. Korean Chem. Soc. 16 (1995), 1180.
5. D. Bao, Z. Wang, W. Ren, L. Zhang, X. Yao. Crystallization kinetics of $Ba_{0.8}Sr_{0.2}TiO_3$ sols and sol-gel synthesis of $Ba_{0.8}Sr_{0.2}TiO_3$ thin films, Ceramics International 25 (1999), 261.
6. H. Miao, Y. Zhou, G. Tan, M. Dong. Microstructure and dielectric properties of ferroelectric barium strontium titanate ceramics prepared by hydrothermal method, J. Electroceram. 21 (2008), 553.
7. V. B. Pavlović, projekat 1832: Sinteza funkcionalnih materijala saglasno tetradi "sinteza-struktura-svojstva-primena", Beograd (2004).
8. H. A. Lotnyk, Solid state reactions in electroceramic systems, Doctoral dissertation, Germany, (2007).
9. B. D. Stojanovic, A. Z. Simoes, C.O. Paiva-Santos, C. Jovalekic, V. V. Mitic, J. A. Varela, Mechanochemical synthesis of bariumtitanate, Journal of the European Ceramic Society 25 (2005) 1985.

Садржај: *Баријум-стронцијум титанат, $Ba_{0.77}Sr_{0.23}TiO_3$, је припремљен од почетних материјала $BaCO_3$, $SrCO_3$ и TiO_2 кроз реакције у чврстом стању. Мешавине ових оксида механички су активирани у високоенергетском планетарном млину у различитим временским интервалима од 0 до 120 минута. У циљу добијања информација о фазном саставу, рендгенском дифракцијом одређена је кристална структура. Уочено је да је након 80 минута дошло до синтезе $Ba_{0.77}Sr_{0.23}TiO_3$. Термалне анализе урађене су са циљем да се одреде карактеристичне температуре процеса који се дешавају у чврстој фази. Расподела величине честица заједно са скенирајућом електронском микроскопијом дале су нам веома корисне информације о морфологији праха.*

Кључне речи: *Механичка активација, скенирајућа електронска микроскопија, кристална структура, баријум-стронцијум титанат.*
